

## Dependence of Argon $K$ -Shell Vacancy Production on the Electronic Structure of Swift Heavy Projectiles\*

Loren M. Winters, James R. Macdonald, Matt D. Brown, Tang Chiao, Louis D. Ellsworth, and E. W. Pettus

*Department of Physics, and Nuclear Science Laboratory, Kansas State University, Manhattan, Kansas 66506*

(Received 25 June 1973)

Thin gas targets of argon were bombarded with C, N, O, and F projectiles of various incident charge states at energies from 1 to 2 MeV/amu. Argon  $K$  x rays were observed with a Si(Li) detector, and x-ray-production cross sections were obtained. For a given-energy projectile, the cross sections decrease approximately exponentially as the number of electrons bound to the incident projectile increases from 0 to 3. For three or more electrons, the measured cross sections change very little. Hartree-Fock calculations of fluorescence yields as a function of target configuration were used to obtain argon  $K$ -shell vacancy-production cross sections. Target configurations were chosen by comparing the experimental argon  $K\alpha$  and  $K\beta$  x-ray energies and  $K\beta/K\alpha$  relative intensities with the values obtained by Hartree-Fock calculations. For projectiles with more than one electron, the vacancy-production cross sections scale as the square of projectile nuclear charge as expected for Coulomb ionization, but the absolute magnitudes of the cross sections do not agree with Coulomb-ionization results. For projectiles with 0 to 1 electron, however, Coulomb ionization alone cannot explain the observed cross sections. Charge exchange from the argon  $K$  shell to projectile bound states has been proposed as a significant vacancy-producing mechanism for collisions involving highly charged projectiles. Although calculations of the charge-exchange cross sections are in reasonable relative agreement with the data, additional vacancy-producing mechanisms cannot be ignored.

### I. INTRODUCTION

Recent experiments<sup>1-3</sup> have shown that the target x-ray production in fast collisions of heavy ions with both gas<sup>1,2</sup> and solid<sup>3</sup> targets is dependent on the initial charge state  $q$  of the projectile. A strong dependence of the target vacancy-production cross section on the nuclear charge  $Z_1$  of the projectile has also been observed<sup>4</sup> for fully stripped projectiles of F, O, N, and C in collisions with argon gas targets. This dependence on nuclear charge is significantly greater than the  $Z_1^2$  dependence of ionization cross sections predicted by existing Coulomb-ionization calculations.<sup>5,6</sup> We have made additional measurements of these charge-dependent effects for carbon, nitrogen, and oxygen projectiles incident on thin argon targets and have confirmed and extended previous measurements<sup>1</sup> of argon  $K$  x-ray-production cross sections for fluorine projectiles. We find that the argon  $K$ -shell vacancy-production cross section increases proportional to  $Z_1^2$  for projectiles with two or more electrons but that the  $Z_1$  dependence strengthens as the number of projectile electrons decreases. For projectiles with less than two electrons, this dependence cannot be explained by direct Coulomb ionization alone. Neither can it be explained in terms of the promotion of argon  $K$ -shell electrons resulting from Pauli exclusion during the collision since the mismatch in the  $K$ -shell levels of target and projectile is so large.<sup>7</sup> It is conceivable, however, that target electrons

in the  $L$  and  $M$  shells may be promoted to higher energy levels by this mechanism when projectiles with  $K$ -shell vacancies enter the collision, thus opening channels for excitation of target  $K$ -shell electrons.

The existence of these charge-dependent effects is clearly important in the interpretation of x-ray data from heavy-ion collisions, particularly for solid targets in which multiple-collision and charge-changing effects may be considerable. Such complications point out the desirability of measuring x-ray yields under single-collision conditions for experiments in which absolute vacancy-production cross sections are determined.

The structure of the target atom poses an additional complication when vacancy-production cross sections are to be extracted from x-ray yields. In violent heavy-ion-atom encounters, multiple vacancies may be produced in the inner as well as the outer shells of the target atoms<sup>8-10</sup> and thus may result in significant changes in fluorescence yields.<sup>11,12</sup> We have attempted to take these changes into account by observing the energy shifts and  $K\beta/K\alpha$  intensity ratios of the argon  $K$  x rays induced by the multiple-vacancy configurations. Although a complete analysis of the effect requires simultaneous detection of x rays and Auger electrons using high-resolution techniques,<sup>12</sup> the procedure we have used is sufficient to indicate that changes in the argon  $K$ -shell fluorescence yield cannot explain the  $Z_1$  and  $q$  dependences of vacancy-production cross sections that we ob-

serve.

McGuire<sup>13</sup> and Halpern and Law<sup>14</sup> have suggested that charge exchange from the Ar *K* shell to bound states of the projectile is a significant vacancy-producing mechanism, particularly for projectiles with only a few electrons. McGuire has performed calculations of this charge exchange using the binary-encounter approximation, whereas Halpern and Law have scaled the Brinkman-Kramers approximation to obtain cross sections. Both results are in reasonable relative agreement with our data; however, they are not conclusive enough to warrant the neglect of other possible vacancy-producing mechanisms. In particular, Coulomb excitation of *K*-shell electrons to vacancies in bound states should not be ignored.

## II. EXPERIMENTAL APPARATUS AND METHODS

Ion beams for the experiment were accelerated by the Kansas State University Tandem Van de Graaff accelerator and momentum analyzed by a 90° bending magnet. C, N, O, and F beams reaching the entrance of the beam-switching magnet passed through a thin carbon foil to produce a distribution of charge states. Each charge state could then be magnetically selected and directed to the entrance of the differentially pumped gas cell (see Fig. 1). The beam current was measured by three Faraday cups located between the first and second apertures, the second and third apertures, and directly behind the fourth aperture. By using these cups, beam transmission through the gas cell could be monitored and maintained at 100%. All three Faraday cups had suppressor rings maintained at -500 V; however, suppression was removed from the first two cups during normal gas-cell operation in order to prevent discharges.

Beam currents typically ranged from 10 to 20 nA for the most probable charge states emerging from the carbon foil, while currents of 1 nA or less were obtained for the least probable charge states. Beam normalization for x-ray yields was achieved by integrating the current from the last Faraday cup.

The beam emerging from the gas cell could alternatively be passed through a magnetic spectrometer and directed onto a position-sensitive detector for charge-state analysis. With residual gas (less than  $5 \times 10^{-5}$  Torr) only in the gas cell, the charge-state purity of the incident beam was always greater than 99%. For purposes of determining x-ray yields, the gas-target thicknesses used were such that less than 5% of the incident beam underwent charge exchange in the gas cell. This prerequisite was also sufficient to ensure

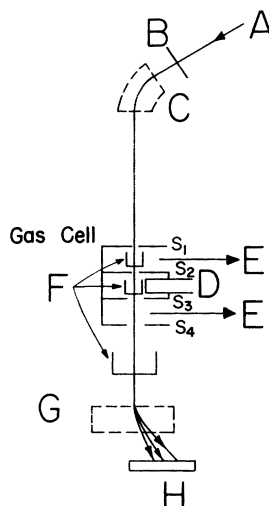


FIG. 1. Experimental apparatus for the measurement of x-ray yields in gases. The components denoted by the letters are: (A) momentum-analyzed beam, (B) charge equilibration foil, (C) magnet for incident charge selection, (D) Si(Li) detector, (E) pumping stations, (F) moveable Faraday cups, (G) magnet for final-charge selection, and (H) position-sensitive detector. The gas-cell aperture sizes are  $S_1 = 1$  mm,  $S_2 = 1.5$  mm,  $S_3 = 2.5$  mm, and  $S_4 = 3$  mm.

single collisions as was indicated by the linear growth of x-ray intensity with target pressure.

X rays were detected by an 80-cm<sup>2</sup> Si(Li) detector placed at right angles to the beam direction. For a given experimental run, the detector was energy calibrated in one or more of the following ways: (i) Mn *K* $\alpha$  and *K* $\beta$  radiation from an <sup>55</sup>Fe source mounted in the gas cell, (ii) electron-induced x-ray production in Mg and Al by an electron gun mounted in the gas cell, and (iii) proton-induced x-ray production in solid targets of Mg, Al, Si, and Cu and gas targets of Ne, Ar, and Kr.

Details of detector operation as well as gas pressure measurement and beam selection are discussed elsewhere.<sup>15</sup> Reference 16 gives details of the system for charge-state analysis.

## III. DATA ANALYSIS

### A. Determination of X-Ray-Production Cross Sections

A typical spectrum of the argon *K* x rays taken under heavy-ion bombardment is shown in Fig. 2. For comparison, the spectrum resulting from proton bombardment is also shown. Both the Ar *K* $\alpha$  and *K* $\beta$  lines are shifted to higher energies for heavy-ion bombardment as compared to proton bombardment. *K* $\alpha$  (peak A) and *K* $\beta$  (peak B) satellite enhancement is expected to contribute substantially to these energy shifts,<sup>8,9</sup> although *K* $\alpha$  hypersatellites<sup>10</sup> may also contribute to peak B. The energy shifts are observed to be dependent on the charge state of the incident projectile, and this fact has been used as a means of choosing appropriate fluorescence yields, a subject to be discussed in Sec. III B. Shifts of 20–100 eV for the *K* $\alpha$  line and 100–250 eV for the *K* $\beta$  line were typical.

The procedures used to extract x-ray yields and x-ray-production cross sections from the spectra have been discussed in a previous publication.<sup>15</sup> It should be noted that the gas cell used for the experiments described in Refs. 1 and 15 was different than the one used in this experiment. Absolute x-ray-production cross sections obtained with the latter gas cell were typically 25% lower than those obtained with the older cell. This discrepancy is likely to be due to improvements resulting from the elimination of beam transmission and pressure measurement problems associated with the older cell. The introduction of increased uncertainty in the solid angle of the newer cell may also contribute to the discrepancy. The latter contribution to uncertainty, which stems from a reduction of the beam-to-detector distance to boost the x-ray counting rate, is estimated at 15% but may be reduced by further investigations of geometrical effects. For purposes of comparing cross sections obtained with the older cell with those taken in the newer, the former cross sections have been reduced by 25% throughout the body of this paper. (This represents an updating of the absolute cross sections of Ref. 4—also obtained with the newer gas cell—for which the heavy-ion x-ray-production cross sections were increased by about 30% in order to make them consistent with cross sections for proton bombardment of argon measured in the older cell. Extensive measurements of proton-induced cross sections have now been performed in the newer cell so that the normalization used in the present work is better.)

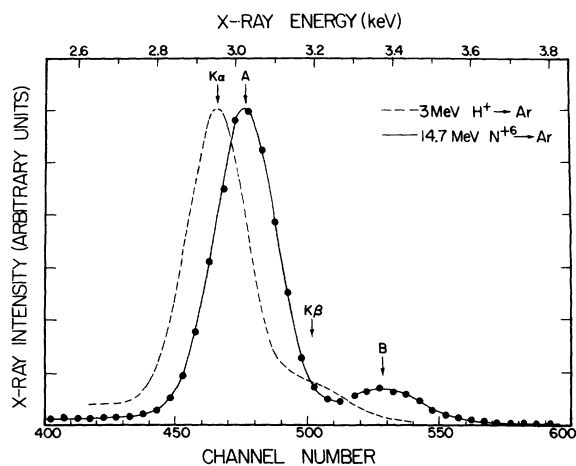


FIG. 2. Typical spectra of the argon  $K$  x-ray lines under proton (dashed line) and heavy-ion (solid line) bombardment. Both spectra have been normalized to the same  $K\alpha$  peak intensity. Peaks A and B are the result of  $K\alpha$  and  $K\beta$  satellite enhancement.

The detector efficiency used to correct the Ar  $K$  x-ray yields for absorption in the 1-mil beryllium window and detector dead layers was 0.86. To obtain the x-ray cross sections, the factor 0.0212 cm was used for the fraction of  $4\pi$  sr subtended by the detector integrated over the interaction length of the target. No correction was made to the data for charge-state impurities in the incident beam or charge exchange in the gas cell since these effects are estimated to result in less than 2% error in the x-ray-production cross sections for a particular charge state.

Contributions to absolute uncertainty not previously discussed are estimated to be 10% from the manometer calibration, 10% from statistics and data-analyzing procedures, and 7% from detector efficiency. The relative uncertainty in the data is estimated at 10%.

#### B. Determination of Vacancy-Production Cross Sections

Since the filling of an inner-shell vacancy can proceed either by radiative or nonradiative means, the x-ray-production cross section for a given shell must be divided by the fluorescence yield for that shell in order to obtain the vacancy-production cross sections. Tables of  $K$ -shell fluorescence yields have been compiled by Bambynek *et al.*<sup>17</sup> for cases where only a single vacancy is produced in the target atom. In violent heavy-ion-atom encounters, however, it is well known that multiple vacancies<sup>8-10</sup> in the target atom may be produced. As a result of these multiple-vacancy configurations, the fluorescence yield of a given shell may be altered substantially. Measurements by Burch *et al.*<sup>11</sup> and Kauffman *et al.*<sup>12</sup> of the  $K$ -shell fluorescence yield of neon under oxygen bombardment are significantly greater than for proton bombardment. Hartree-Fock calculations by Bhalla and Hein<sup>18</sup> are in reasonable agreement with these measurements.

Bhalla<sup>19</sup> has performed Hartree-Fock calculations of Ar  $K$ -shell fluorescence yields as a function of the number of  $2p$  and  $3p$  vacancies. Moreover, he has calculated the  $K\alpha$  and  $K\beta$  energies as well as the  $K\beta/K\alpha$  relative-intensity ratios for the various configurations. These calculations allow one to systematically select an effective fluorescence yield to determine the vacancy-production cross sections. The following method has been adopted to do this.

For each projectile of charge state  $q$  and energy  $E$ , the experimental argon  $K\alpha$  and  $K\beta$  x-ray energies and  $K\beta/K\alpha$  relative intensities were compared to Bhalla's calculations in order to choose target configurations. In many cases, experimental uncertainties made it impossible to choose a

TABLE I. Average argon  $K$ -shell fluorescence yields calculated from Ref. 19. Also given are the experimental energy shifts  $\Delta E(K\alpha)$  and  $\Delta E(K\beta)$  of the argon  $K\alpha$  and  $K\beta$  lines, respectively, as well as the experimental  $K\beta/K\alpha$  relative intensities. All defect configurations consistent with these measured energy shifts and ratios are given for each projectile of nuclear charge  $Z_1$  and incident charge state  $q$ .

$Z_1$	$q$	$\Delta E(K\alpha)$ (eV)	$\Delta E(K\beta)$ (eV)	$K\beta/K\alpha$ relative intensity	$\bar{\omega}_K$	Defect configurations ( $1s, 2p^m, 3p^n$ )	
						$m$	$n$
1	1	0	0	...	0.120	0	0
6	3	45	119	0.13	0.137	2	2, 3
	4	48	139	0.145	0.141	2	2, 3 3 3, 4
5	52	139	0.145	0.141	2	2, 3 3 3, 4	
	6	54	156	0.13	0.146	3	3, 4
7	3	54	139	0.14	0.146	3	2, 3, 4
	4	57	...	0.15	0.146	3	2, 3, 4
5	59	144	0.15	0.146	3	2, 3, 4	
	65	159	0.145	0.146	3	3, 4	
7	70	185	0.135	0.147	3	3, 4	
	8	77	233	0.13	0.148	3	3, 4 4 4, 5
9	4	22	134	0.12	0.137	2	2, 3
	5	45	160	0.12	0.140	2	2, 3 3 4
6	59	168	0.13	0.146	3	3, 4	
	61	178	0.14	0.146	3	3, 4	
8	73	196	0.14	0.148	3	3, 4 4 4, 5	
	93	246	0.15	0.150	4	4, 5	

unique fluorescence yield corresponding to a single-target configuration. Even in such cases, however, the fluorescence yields corresponding to the possible configurations often varied by less than 1% and never more than 7%. Similar variations in possible fluorescence yields were shown for the various energies of a given projectile-charge-state combination. This latter fact, coupled with the uncertainty of  $\sim 20$  eV in the x-ray-energy calibration for the low-energy fluorine and the oxygen data, made it undesirable to obtain values of the fluorescence yields (to be used in determining vacancy-production cross sections) as a function of bombarding energy. Instead, these values were obtained by averaging the fluorescence yields for all chosen configurations of a given projectile-charge-state system.

The average fluorescence yields obtained and the configurations which are consistent with the experimental measurements are given in Table I. Also given are the experimental  $K\alpha$  and  $K\beta$  energy shifts relative to the corresponding proton-induced transitions and the  $K\beta/K\alpha$  relative intensities. These values are also averages of the values at all energies of a given projectile-charge-state combination. The experimental uncertainty in these average values are about 10 eV for the Ar  $K\alpha$  line, 30 eV for the Ar  $K\beta$  line, and 0.02 for the  $K\beta/K\alpha$  relative intensities.

In a previous experiment,<sup>4</sup> fluorescence yields for the Ar  $K$  shell that were obtained by Larkins<sup>20</sup> in the statistical approximation using calculations of McGuire (see Ref. 20) were used. A comparison

TABLE II. Argon  $K$ -shell x-ray-production and vacancy-production cross sections for projectiles with nuclear charge  $Z_1$ , energy  $E$ , and  $n$  bound electrons.

$Z_1$	$E$ (MeV)	X-ray-production cross section ( $10^{-20}$ cm <sup>2</sup> )					Vacancy-production cross section ( $10^{-20}$ cm <sup>2</sup> )							
		$n:$	0	1	2	3	4	5	0	1	2	3	4	5
1	1.05		0.0136						0.113					
	1.58		0.0261						0.218					
	1.87		0.0329						0.274					
6	12.6		0.623	0.383	0.270	0.217			4.27	2.72	1.91	1.58		
	18.0		1.71						11.7					
	22.6		2.21	1.50	1.09				15.1	10.6	7.73			
7	14.7		0.963	0.564	0.387	0.261	0.259		6.55	3.86	2.65	1.79	1.77	
	21.0		2.58						17.6					
	26.3		3.80	2.26	1.45				25.9	15.5	9.93			
8	16.8		1.74						11.8					
	24.0		4.30						29.0					
	30.0		5.79	3.27					39.1	24.0				
9	20.0		3.46	1.48	0.666	0.422	0.410	0.393	23.1	10.0	4.56	2.89	2.93	2.87
	30.0		7.63	3.85	1.86	1.19			50.9	26.0	12.7	8.15		
	35.5		9.17	5.03	2.66	1.66			61.1	34.0	18.2	11.4		

of these yields with those given in Table I for the fully stripped projectiles reveals differences of less than 25% in all cases. Such deviations result in an alteration of the vacancy-production cross sections but do not change the general trends of the data.

From the table, one can see that the argon fluorescence yields vary by less than 10% for the different heavy-ion projectiles. This variation is quite small compared to the many-fold changes observed with different charge states for the x-ray-production cross sections and cannot explain these changes.

#### IV. RESULTS AND DISCUSSION

The experimental Ar K x-ray-production and vacancy-production cross sections for incident projectiles with energy  $E$  and  $n$  bound electrons are given in Table II. Included in this table are previously published<sup>4</sup> cross sections for fully stripped projectiles incident on argon. These latter cross sections are useful in examining the projectile energy dependence of vacancy production.

Experimental Ar K x-ray-production cross sections obtained with different incident charge states at several energies are plotted in Fig. 3 for O, N,

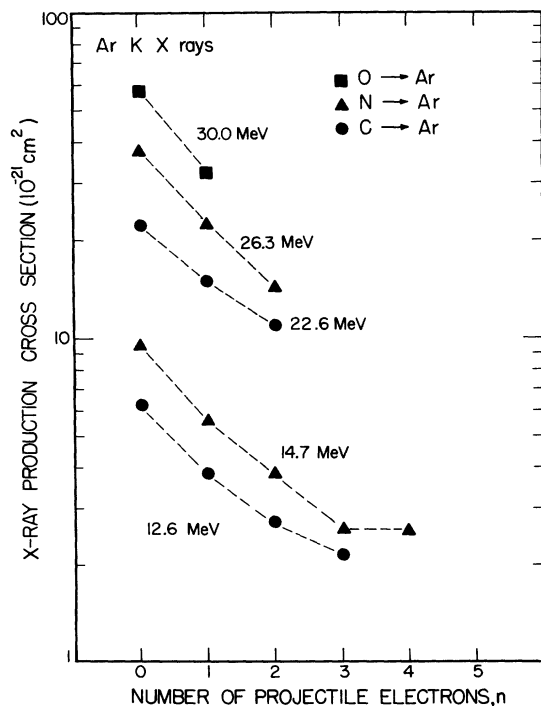


FIG. 3. Argon K x-ray-production cross sections as a function of the number of projectile electrons  $n$  for C, N, and O projectiles. The dashed lines are drawn to guide the eye.

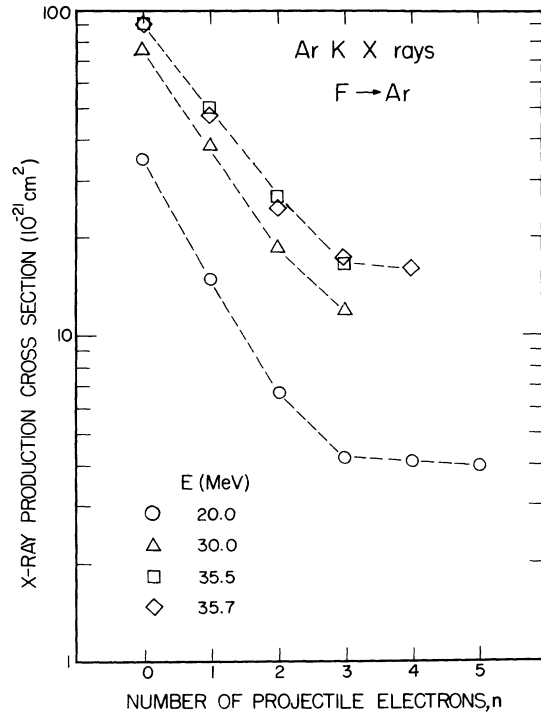


FIG. 4. Argon K x-ray-production cross sections as a function of the number of projectile electrons  $n$  for fluorine projectiles at four energies. The open diamonds represent data from Ref. 1. They have been reduced by 25% (as described in the text) to allow relative comparison with the data at 35.5 MeV (open squares). The dashed lines are drawn to guide the eye.

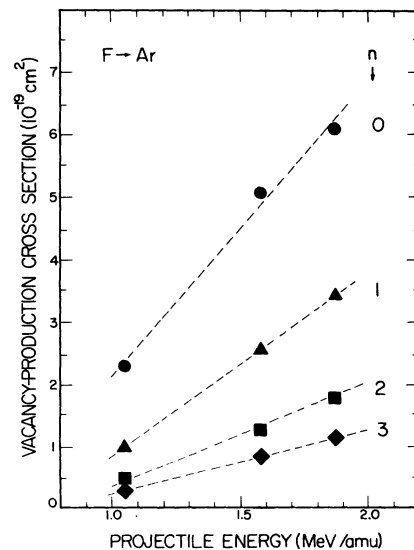


FIG. 5. Argon K-shell vacancy-production cross sections as a function of the energy of fluorine projectiles with  $n$  bound electrons. The dashed lines are linear least-squares fits to the data for each  $n$ .

and C projectiles. As the number of projectile electrons increases from zero to three, an almost exponential decrease in the cross sections is observed. For three or more projectile electrons, an approximately constant value of the cross section is exhibited. These trends are consistent with those of previous data<sup>1</sup> taken with 35.7-MeV fluorine projectiles incident on argon.

From the data shown in Fig. 4 for 20-, 30-, and 36-MeV fluorine projectiles incident on argon, the rapid increase in cross sections with decreasing projectile electron number is clearly greatest at the lowest projectile energy. At 35.5 MeV, a fivefold increase in cross sections is observed between  $n=3$  and  $n=0$ , while at 20 MeV, the increase is eightfold. This enhancement of the charge-state dependence at lower energy may be indicative of the importance of electron promotion processes at these energies. Such processes include molecular excitations described by the Fano-Lichten model,<sup>7</sup> charge exchange, and possibly multiple excitations in the same small-impact-parameter collision.

For  $n < 3$ , the approximate exponential increase in cross sections is, by itself, sufficient to suggest that electron-promotion processes associated with  $1s$  vacancies in the projectile compete favorably with Coulomb ionization in producing argon  $K$ -shell vacancies. This possibility may be investigated further by comparing the experimental

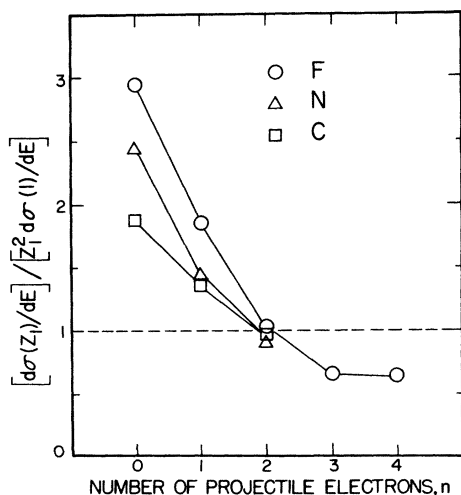


FIG. 6. Normalized differential-cross-section ratio  $[d\sigma(Z_1)/dE]/[Z_1^2 d\sigma(1)/dE]$  as a function of the number of projectile electrons  $n$ .  $\sigma(Z_1)$  is the argon  $K$ -shell vacancy-production cross section for a projectile of nuclear charge  $Z_1$  and  $\sigma(1)$  is the corresponding cross section for proton bombardment.  $E$  is the projectile energy in units of MeV/amu. The dashed line is the result obtained for Coulomb ionization. The solid lines are drawn to guide the eye.

vacancy-production cross sections with those expected for Coulomb ionization.

The Ar  $K$  vacancy-production cross sections for the F-Ar system are plotted in Fig. 5 for the various projectile electron numbers as a function of projectile energy in units of MeV/amu. The data for a given  $n$  appear to exhibit a linear energy dependence and have been fitted with a linear least-squares routine (indicated by dashed lines). A linear energy dependence has also been assumed for the data at  $n=4$  which is not shown in Fig. 5 since it overlaps the data at  $n=3$ . The differential vacancy-production cross sections  $d\sigma/dE$ , given by the slopes of these fits, exhibit a striking dependence on  $n$ . In a similar way as with the x-ray-production cross sections, the  $d\sigma/dE$  values show a rapid decrease for  $n < 3$  but apparently level off for  $n \geq 3$  to a value of  $d\sigma/dE$  in the vicinity of the result obtained by a  $Z_1^2$  scaling of the value  $d\sigma(1)/dE$  measured for proton bombardment of argon in the same velocity region. In particular, the energy dependence of cross sections for  $n=2$  does scale with  $Z_1^2$  and hence agrees with the Coulomb-ionization result.

Values of  $d\sigma/dE$  have also been obtained for C and N for  $n \leq 2$  by assuming linear energy dependences of their cross sections. A normalization of these values to the result obtained from a  $Z_1^2$  scaling of  $d\sigma(1)/dE$  allows a comparison to Coulomb ionization as shown in Fig. 6. The differential cross section  $d\sigma(Z_1)/dE$  for a projectile of nuclear charge  $Z_1$  has been divided by the Coulomb-ionization result  $Z_1^2 d\sigma(1)/dE$  and this ratio has been plotted versus  $n$ . If the energy dependence of Coulomb ionization were valid, all the data should fall on the dashed line at unity. This is certainly the case at  $n=2$ , but marked deviations from unity occur for  $n < 2$ . For  $n > 2$ , the normalized differential cross section is still falling but changes very little from  $n=3$  to  $n=4$ . The departure from Coulomb ionization at  $n=0$  and 1 again suggests the importance of electron promotion processes associated with  $1s$  projectile vacancies. For  $n > 2$ , Coulomb ionization dominates the vacancy-production process, but charge-state and energy-dependent corrections to the process may be necessary. At  $n=2$ , Coulomb ionization explains the energy dependence of vacancy production remarkably well for these projectiles in the energy range of concern.

Deviations from the  $Z_1^2$  scaling law can also be examined for the absolute vacancy-production cross sections. In Fig. 7, the normalized cross-section ratio  $\sigma(Z_1)/Z_1^2 \sigma(1)$  is plotted as a function of  $n$  for the four projectiles. As for the differential cross sections, this ratio should be unity if Coulomb ionization describes the vacancy-pro-

duction process. Again, this is not the case. The ratios are significantly greater than unity for low values of  $n$ , crossover unity at intermediate values of  $n$ , and are significantly less than unity at high values of  $n$ . This behavior is similar to that observed for the differential cross-section ratios and suggests the same interpretation.

It is possible, however, to proceed a step further in the interpretation and examine the cross-section ratios as a function of  $Z_1$  for the various values of  $n$ . Such a plot is shown in Fig. 8 for the two energies 1.05 and 1.87 MeV/amu. From this figure it is clear that for  $n \geq 2$ , agreement with  $Z_1^2$  scaling is good for the C, N, O, and F projectiles as a closed group but that none of these projectiles scale as  $Z_1^2$  with protons since the normalized cross sections are less than unity. If, however,  $Z_1$  is replaced by a screened nuclear charge  $Z_1' = Z_1 - Z_1 \zeta(E, n)$ , where  $\zeta$  is a screening number which depends on  $E$  and  $n$  but not on  $Z_1$ , then it is possible, for  $n=2$  and 3 to choose values of  $\zeta$  such that  $\sigma(Z_1)/(Z_1')^2 \sigma(1) = 1$  as one might expect from Coulomb ionization. The ratio  $\zeta Z_1/n$  has been formed in order to compare the reduction in nuclear charge required by this screening model with the number of projectile electrons available for screening. These ratios extend from about 0.6 to 1.3 and are clearly much too large to permit this model to account for the deviations of

the vacancy-production cross sections from  $Z_1^2$  scaling with protons. This is not to say that screening does not account for some of the deviation, but rather that additional energy-dependent and  $n$ -dependent corrections to Coulomb ionization must be considered. For  $n=0$  and 1, however, it is evident from Fig. 8 that vacancy-production mechanisms other than Coulomb ionization are more important.

McGuire<sup>13</sup> and Halpern and Law<sup>14</sup> have shown that inclusion of the additional mechanism of charge exchange from the Ar  $K$  shell to projectile bound states gives a reasonable accounting for our experimental vacancy-production cross sections for fully stripped projectiles.<sup>4</sup> McGuire's calculations are done in the framework of the binary-encounter approximation, whereas Halpern and Law have performed a scaling of the Brinkman-Kramers approximation for the process in order to fit our data. McGuire has made additional calculations of vacancy-production cross sections for the 35.7-MeV F-Ar collision as a function of  $q$ . These results are also in fair agreement with the data.

We have used yet another method to estimate the contribution to vacancy production of electron capture from the target  $K$  shell to projectile levels. In this method, the Brinkman-Kramers approximation for electron capture from the argon

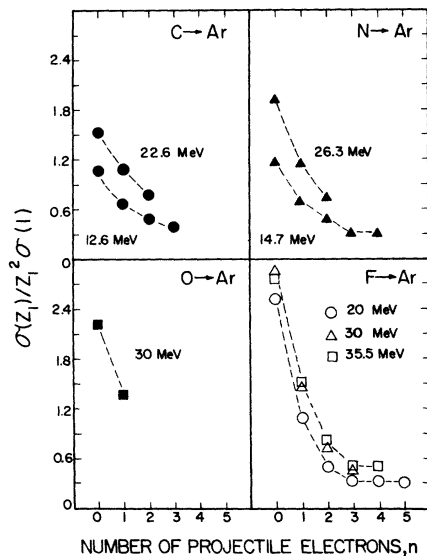


FIG. 7. Normalized cross-section ratio  $\sigma(Z_1)/Z_1^2 \sigma(1)$  as a function of the number of projectile electrons  $n$  for C, N, O, and F projectiles of various energies.  $\sigma(Z_1)$  is the argon  $K$ -shell vacancy-production cross section for a projectile of nuclear charge  $Z_1$  and  $\sigma(1)$  is the corresponding cross section for protons of the same velocity. The dashed lines are drawn to guide the eye.

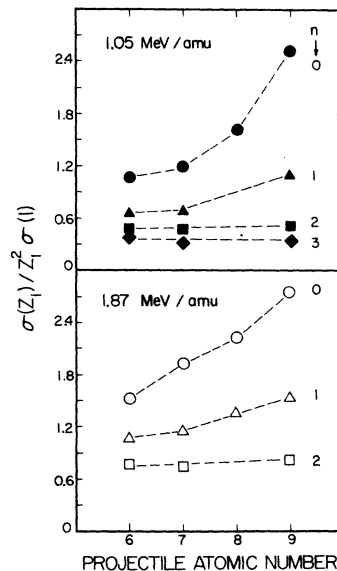


FIG. 8. Normalized cross-section ratio  $\sigma(Z_1)/Z_1^2 \sigma(1)$  as a function of projectile nuclear charge for two velocities of projectiles with  $n$  bound electrons.  $\sigma(Z_1)$  is the argon  $K$ -shell vacancy-production cross section for a projectile of nuclear charge  $Z_1$  and  $\sigma(1)$  is the corresponding cross section for protons of the same velocity. The dashed lines are drawn to guide the eye.

*K* shell to incident protons as given by Nikolaev<sup>21</sup> is used. This result is then scaled to the projectiles of interest using Nikolaev's empirical scaling formula for heavy-ion electron-capture cross sections.<sup>22</sup> For fully stripped projectiles of F, O, N, and C at 1.9 MeV/amu, the *K*-shell electron-capture contribution to vacancy-production estimated by this method is about 30% of the measured cross sections. There is, of course, considerable uncertainty in this procedure. For example, experimental measurements<sup>23</sup> of cross sections for electron capture from all shells for 36-MeV F<sup>9+</sup> on argon are only one-third as large as the values obtained by using the scaling procedure. Nevertheless, this method is sufficient to indicate that charge exchange from the argon *K* shell does not, by itself, explain the deviations from Coulomb ionization exhibited by the vacancy-production cross sections for  $n=0$  and 1.

We suggest that *K*-shell charge exchange may be only one of a number of mechanisms which enhance the *K*-shell vacancy production. These mechanisms involve the promotion of target electrons early in the collision, thus opening channels with large excitation cross sections for target *K*-shell electrons to bound states. The formation of these channels may be expected to depend on the occupation of the projectile *K* shells, with more channels opening as the number of projectile *K* electrons decreases. For example, results of calculations of excitation and ionization of hydrogen by H and H<sup>+</sup> impact are given by Mott and Massey.<sup>24</sup> The excitation cross sections for these systems are comparable to the ionization cross sections; moreover, excitation and ionization by neutral hydrogen impact is significantly lower than by proton impact. Similar calculations for

excitation of targets of higher atomic number may be useful in interpreting projectile structure effects in heavy-ion-atom collisions.

#### V. SUMMARY

We have examined the dependence of Ar *K*-shell vacancy-production cross sections on the initial charge state of carbon, nitrogen, oxygen, and fluorine projectiles in the energy range of 1–2 MeV/amu. Large increases in these cross sections and the projectile energy dependences of the cross sections are observed as a function of projectile nuclear charge  $Z_1$  and projectile electron number  $n$  for  $n < 2$ . For  $n \geq 2$ , Coulomb ionization can account for the data if  $n$ -dependent and energy-dependent corrections (such as electron screening of the projectile) are applied. For  $n=0$  and 1, however, other mechanisms must be invoked to explain the large increases in the cross sections. Charge exchange from the argon *K* shell to projectile bound states is one such mechanism, and is included in processes which involve excitation of target *K*-shell electrons to bound states left unoccupied by electron promotion early in the collision. We suggest that theoretical investigations of such excitation processes be made in order to aid the interpretation of these heavy-ion-atom collisions.

#### ACKNOWLEDGMENTS

The authors wish to acknowledge the courtesy of Dr. Chander Bhalla in making his calculations of fluorescence yields available prior to publication. Thanks are also extended to Dr. James H. McGuire for many helpful discussions.

\*Work partially supported by the U. S. Atomic Energy Commission under Contract No. AT(11-1)-2130.

<sup>1</sup>James R. Macdonald, Loren Winters, Matt D. Brown, Tang Chiao, and Louis D. Ellsworth, *Phys. Rev. Lett.* **29**, 1291 (1972).

<sup>2</sup>J. Richard Mowat, D. J. Pegg, R. S. Peterson, P. M. Griffin, and I. A. Sellin, *Phys. Rev. Lett.* **29**, 1577 (1972); J. Richard Mowat, I. A. Sellin, D. J. Pegg, R. S. Peterson, Matt D. Brown, and James R. Macdonald, *Phys. Rev. Lett.* **30**, 1289 (1973).

<sup>3</sup>Werner Brandt, Roman Laubert, Manuel Mourino, and Arthur Schwarzschild, *Phys. Rev. Lett.* **30**, 358 (1973).

<sup>4</sup>J. R. Macdonald, L. M. Winters, M. D. Brown, L. D. Ellsworth, T. Chao, and E. W. Pettus, *Phys. Rev. Lett.* **30**, 251 (1973).

<sup>5</sup>E. Merzbacher and H. W. Lewis, in *Handbuch der Physik*, edited by S. Flügge (Springer, Berlin, 1958), Vol. 34, p. 166.

<sup>6</sup>J. D. Garcia, *Phys. Rev. A* **1**, 280 (1970); *Phys. Rev. A* **1**, 1402 (1970).

<sup>7</sup>U. Fano and W. Lichten, *Phys. Rev. Lett.* **14**, 627 (1965); William Lichten, *Phys. Rev.* **164**, 131 (1967); M. Barat and W. Lichten, *Phys. Rev. A* **6**, 211 (1972).

<sup>8</sup>Patrick Richard, I. L. Morgan, T. Furuta, and D. Burch, *Phys. Rev. Lett.* **23**, 1009 (1969); D. Burch and Patrick Richard, *Phys. Rev. Lett.* **25**, 983 (1970).

<sup>9</sup>A. R. Knudson, D. J. Nagel, P. G. Burkhalter, and K. L. Dunning, *Phys. Rev. Lett.* **26**, 1149 (1971).

<sup>10</sup>P. Richard, W. Hodge, and C. F. Moore, *Phys. Rev. Lett.* **29**, 393 (1972).

<sup>11</sup>D. Burch, W. B. Ingalls, J. S. Risley, and P. Heffner, *Phys. Rev. Lett.* **29**, 1719 (1972).

<sup>12</sup>R. L. Kauffman, F. Hopkins, C. W. Woods, and P. Richard (unpublished).

<sup>13</sup>J. H. McGuire (unpublished); also, private communication.

- <sup>14</sup>A. M. Halpern and J. Law, *Phys. Rev. Lett.* 31, 4 (1973).
- <sup>15</sup>Loren M. Winters, James R. Macdonald, Matt D. Brown, Louis D. Ellsworth, and Tang Chiao, *Phys. Rev. A* 7, 1276 (1973).
- <sup>16</sup>J. R. Macdonald, S. M. Ferguson, T. Chiao, L. D. Ellsworth, and S. A. Savoy, *Phys. Rev. A* 5, 1188 (1972).
- <sup>17</sup>W. Bambynek, B. Crasemann, R. W. Fink, H. V. Freund, H. Mark, C. D. Swift, R. E. Price, and P. Venugopala Rao, *Rev. Mod. Phys.* 44, 716 (1972).
- <sup>18</sup>C. P. Bhalla and M. Hein, *Phys. Rev. Lett.* 30, 39 (1973).
- <sup>19</sup>C. P. Bhalla, *Phys. Rev. A* (to be published).
- <sup>20</sup>F. P. Larkins, *J. Phys. B* 4, L29 (1971); E. J. McGuire, *Phys. Rev.* 185, 1 (1969); *Phys. Rev. A* 2, 273 (1970).
- <sup>21</sup>V. S. Nikolaev, *Zh. Eksp. Teor. Fiz.* 51, 1263 (1966) [*Sov. Phys.-JETP* 24, 847 (1967)].
- <sup>22</sup>V. S. Nikolaev, *Usp. Fiz. Nauk* 85, 679 (1965) [*Sov. Phys. Usp.* 8, 629 (1965)].
- <sup>23</sup>S. M. Ferguson, J. R. Macdonald, T. Chiao, L. D. Ellsworth and S. A. Savoy, *Phys. Rev. A* (to be published).
- <sup>24</sup>N. F. Mott and H. S. W. Massey, *The Theory of Atomic Collisions*, 3rd ed. (Clarendon, Oxford, 1965), p. 615.